encit 2022

ABCM Associação Brasileira de Engenharia e Ciências Mecânicas

19th Brazilian Congress of Thermal Sciences and Engineering
November 6th–10th, 2022, Bento Gonçalves - RS - Brazil

# ENC-2022-0003
# DYNAMIC ANALYSIS OF PRESSURIZATION OF CONTAINMENT BUILDING OF A PRESSURIZED WATER REACTOR WITH PHASE CHANGE MATERIALS

**Rafaela Vilas Boas Pedrassani**
**Jian Su**
COOPE, Federal University of Rio de Janeiro - Nuclear Engineering Program
rafaela.pedrassani@coppe.ufrj.br ; sujian@coppe.ufrj.br

***Abstract.*** *Pressurization of the containment building of a pressurized water reactor nuclear power plant can occur in a short time if a loss of coolant accident (LOCA) occurs due to a break in the primary circuit piping. Recently, phase change materials (PCM) have been considered as a method of passive cooling in the containment building by storing thermal energy in case of accidents. This paper reports a coupled model for the PWR containment pressurization during a LOCA based on Hermite approximations for integrals. It consists of a conservative single-cell thermodynamic model for the mass and energy balance in the containment, and an improved lumped parameter model for one-dimensional heat conduction with the melting of PCM slabs. The nonlinear system of ordinary differential equations is solved numerically using the symbolic-numerical software Wolfram Mathematica 11.0. The containment model is verified by comparing the final containment pressure and temperature with available literature data. On the other hand, the PCM heat conduction model is validated by comparing its melting interface and liquid phase average temperature with an approximate analytical solution. Temperature and pressure variations in the containment were evaluated for different types and heat transfer areas of the PCM. The analysis results demonstrated that the PCM could successfully cool the containment and attenuate the pressure rise.*

***Keywords:*** *Reactor containment, phase change material, thermal energy storage, heat conduction, lumped models*

## 1. INTRODUCTION

The containment building of a pressurized water reactor (PWR) is designed to meet the requirements of structural integrity under the hypothetical loss of coolant accident (LOCA), withstanding the pressurization due to the primary coolant evaporation. In recent years, phase change materials (PCM) have been considered a passive cooling method for the reactor containment building due to the considerable latent heat during the phase change process.

Thermal-hydraulic behavior of the containment during a large break loss of coolant accident (LBLOCA) has been investigated by several studies. Noori-Kalkhoran *et al.* (2014) analyzed the thermo-hydraulic parameters of the Bushehr Nuclear Power Plant during a double-ended cold leg accident (DECL). They used the CONTAIN 2.O code, developed by the Sandia Laboratory in 1997. Lee and Fan (2017) analyzed the pressurization and combustion of combustible gases in a PWR containment building during a power outage sequence at the power plant and used the CONTAIN, MARCH3 and MAAP codes to simulate the thermo-hydraulic parameters of the reactor and the containment structure. Papini *et al.* (2011) investigated the condensation, pressure and temperature phenomena involved in the containment of the International Reactor Innovative and Secure (IRIS) using the GOTHIC and RELAP5 codes. The IRIS containment was implemented with RELAP5, based on the concept of two jointed tubes, while the GOTHIC code used several modeling options for heat transfer correlations and thermal structure nodalization. Avelar *et al.* (2020) presented a simplified model for post-inertization of the containment of a small modular reactor (SMR) to mitigate the risk of hydrogen detonation, under the conservative hypothesis of a LOCA followed by complete failure of the reactor emergency cooling system.

Saeed *et al.* (2019) presented a characterization of high-temperature PCMs to improve passive safety and heat removal capabilities in nuclear reactor systems. Cho *et al.* (2021) studied a system to act as final heat sinks for containment. In addition, an experiment was designed to verify the real heat absorption capacity of the PCM of different geometries. The results showed that even without the spray systems in the containment, the proposed condensers could successfully cool it.

In this study, we propose a coupled model for the PWR containment pressurization during a hypothetical LOCA.

The proposed model, based on Hermite approximations for integrals, consists of a conservative single-cell thermodynamic model for the mass and energy balance in the containment, and an improved lumped parameter model for one-dimensional heat conduction with the melting of PCM slabs. The nonlinear system of ordinary differential equations is solved numerically using the symbolic-numerical software Wolfram Mathematica 11.0.

## 2. METHODOLOGY

The installation of PCM slabs in a PWR containment building is proposed to act as the final heat sink to absorb the heat released by the evaporation of the primary coolant during a LOCA, as shown in Fig 1. As a simple system, this PCM condenser does not need to modify the containment wall for installation. Thus, it can be applied in operating PWR plants and work with other passive cooling systems to improve cooling efficiency.

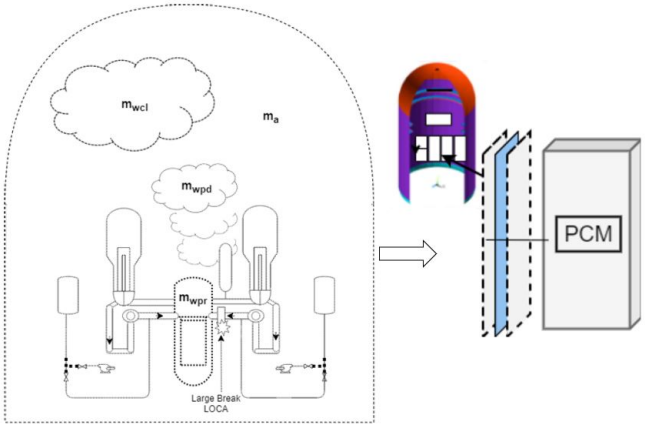


Figure 1. Illustration of the containment building of a PWR nuclear power plant with PCM slabs.

### 2.1 Thermodynamic model

A conservative single-cell thermodynamic model for the mass and energy balance in the containment is proposed by Todreas and Kazimi (2012). The thermodynamic system of interests is composed of three subsystems: containment air of mass $m_a$, water vapour initially in the air of the containment $m_{wcl}$, and water initially in the primary system $m_{wp}$. At any given time, of the mass $m_{wp}$, the portion $m_{wpd}$ has discharged into the containment and the portion $m_{wpr}$ remains in the primary system. The total water inventory in the primary system is written as $m_{wp} = m_{wpd} + m_{wpr}$.

For the analysis of the transient conditions, the first law of thermodynamics is written as:

$$\frac{d}{dt}(m_a u_a + m_{wcl} u_{wcl} + m_{wpd} u_{wpd} + m_{wpr} u_{wpr}) = \dot{Q}_{n-wpr} - \sum_i \dot{Q}_{i-st}, \tag{1}$$

where $\sum$ represents the subsystems that comprise the containment atmosphere and $u$ represents the specific internal energy. The subscripts $a$, $wcl$, $wpd$, $wpr$, $n$ and $st$ refer to air, initial containment water, coolant discharged from the primary system, coolant remaining in the primary system, core fuel, and structures, respectively. $\dot{Q}_{wpr-c}$ is the rate of heat transferred from water remaining of the primary system to control volume and $\dot{Q}_{c-st}$ is the rate of heat transferred from control volume to structures.

The first law for the control volume is rewritten using the total energy $U_{c.v.}$:

$$\dot{U}_{c.v.} = \dot{m}(t) h_p(t) + \dot{Q}_{wpr-c} - \dot{Q}_{c-st}, \tag{2}$$

where $h_p$ and $\dot{m}(t)$ are the specific enthalpy and mass flow rate of the primary coolant.

The water mass balance in the containment atmosphere is given by:

$$\frac{dm_w(t)}{dt} = \dot{m}(t), \tag{3}$$

where $m_w$ refers to the total mass at operating conditions.

With regards to the energy balance, the following assumptions are applied: negligible potential energy and no external work is added to the system by e.g. pumps. Then, the energy balance of the system may be expressed in terms of the internal energy $U$ over a time step $\Delta t$:

$$U^{t+\Delta t} = U^t + \int_t^{t+\Delta t} h_p(t)\dot{m}(t)dt + \dot{Q}_{wpr-c}\Delta t - \dot{Q}_{c-st}\Delta t, \tag{4}$$

where:
$U^{t+\Delta t} = m_a u_a^{t+\Delta t} + (m_{wcl}^t + m_{wpd}^{t+\Delta t}) u_{wcl}^{t+\Delta t}$,
$U^t = m_a u_a^t + m_{wcl} u_{wcl}^t$.

The heat loss ($Q_{wpr-c}$) has been neglected in this model.

The internal energy of the system $U$ is related to the system enthalpy $H$, and assuming constant pressure $P$ throughout the containment volume $V$ by the following relation:

$$H(P,T) = U(P,T) + PV. \tag{5}$$

Eqs. (3 - 5) with the equation of state of the water are sufficient to solve for the four main unknowns: the total fluid mass $m_w$, the total fluid enthalpy $H$, the total fluid internal energy $U$ and the pressure $P$. From these, all other variables of interest can be determined.

### 2.2 Equilibrium pressure conditions

Analysis of equilibrium pressure conditions is achieved upon establishment of pressure equilibrium between the containment and the primary system. The energy balance of Eq. (4) may thus be expressed as:

$$m_w(u_w^{t+\Delta t} - u_w^t) + m_a c_{va}(T_c^{t+\Delta t} - T_a^t) = \dot{Q}_{wpr-c}\Delta t - \dot{Q}_{c-st}\Delta t, \tag{6}$$

where $c_{va}$ is the specific heat of air at constant volume, $T_c$ the mixture temperature in the containment and $T_a$ the dry bulb temperature.

Equation (6) can be rewritten to express the water conditions separately as primary system and water in the air:

$$m_{wpd}^{t+\Delta t}(u_f^{t+\Delta t} + x_{st} u_{fg}^{t+\Delta t}) + m_{wa}^t(u_f^{t+\Delta t} + x_{st} u_{fg}^{t+\Delta t}) + m_a C_{va}(T_c^{t+\Delta t}) = U^{t+\Delta t}, \tag{7}$$

where $u$ and $v$ are the specific internal energy and specific volume, respectively, all as functions of $T_c^{t+\Delta t}$. The subscript $f$ refers to water, $g$ refers to vapour and $fg$ refers to evaporation.

Introducing the definition of the steam static quality $x_{st}$ in the containment and assuming air as an perfect gas, the following equation is obtained:

$$x_{st} = \frac{\frac{V_T}{m_w^{t+\Delta t}} - v_f^{t+\Delta t}}{v_{fg}^{t+\Delta t}}, \tag{8}$$

where $V_T$ is the total volume and can be calculated by using the containment free volume $V_c$ and the volume of primary system $V_p$, written as $V_T = V_c + V_p$.

The total pressure is obtained by assuming that the vapour phase obeyed the Dalton's law. The total pressure exerted by vapour phase equals the sum of the partial pressures:

$$P^{t+\Delta t} = P_{wa}^{t+\Delta t} + P_a^{t+\Delta t}, \tag{9}$$

where $P^{t+\Delta t}$ is the pressure of mixture, $P_{wa}^{t+\Delta t}$ is the partial pressure of the saturated water vapour corresponding to $T_c^{t+\Delta t}$ and $P_a^{t+\Delta t}$ is the partial pressure of air corresponding to $T_c^{t+\Delta t}$.

Considering each mixture component occupies the total volume, the following equation is obtained:

$$V_T^{t\Delta t} = \sum_{t=1}^{t+\Delta t} (m_{wpd}^t v_{wpd}^t) + V_c. \tag{10}$$

The initial conditions are stated in terms of relative humidity $\phi$, the dry bulb temperature $T_a$ and the total pressure $P^{t+\Delta t}$. From the definition of relative humidity, the saturated vapour pressure $P_{wa}^t$ can be expressed as:

$$P_{wa}^t = \phi p_{sat}(T_a^t), \tag{11}$$

where $sat$ refers to saturation condition.

The containment air of mass is given by the equation of state for a perfect gas:

$$m_a = \frac{P_a^0 V_c}{R_a T_a^0}, \tag{12}$$

where $P_a$ is the partial pressure of the saturated water vapour and $R_a$ is the universal gas constant.

The containment mass of water can be expressed as:

$$m_{wa}^0 = \frac{V_c}{v_{wa}^0}, \tag{13}$$

where $v_{wa}$ is the specific volume of water vapour.

And the total mass is given by:

$$m_w^{t\Delta t} = \sum_{t=1}^{t+\Delta t} (m_{wpd}^t + m_{wa}^0) \tag{14}$$

Now, all of the unknown parameters depend on $T_c(t)$. By combining mass flow and enthalpy, the solution algorithm to calculate containment temperature and pressure variation with respect to the time can be determined, based on the assumption that the non-condensible gas and water steam are homogeneous and in thermal equilibrium.

### 2.3 PCM melting process

Consider the melting process of a PCM slab with thickness $2a$. Assuming symmetry with respect to the middle plane of the slab, only a half of the PCM slab is analyzed, as shown in Fig 2.

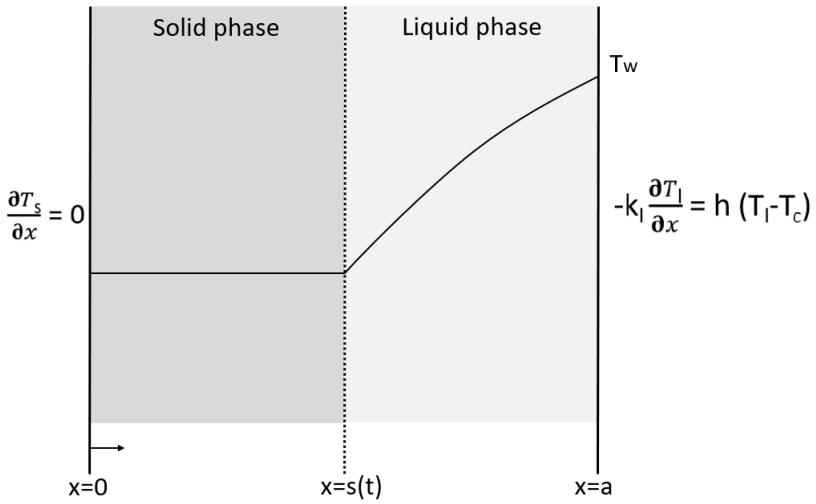


Figure 2. Illustration of one-dimensional melting process in a symmetric PCM slab.

The analytical model is based on the following assumptions: 1) One-dimensional melting model and no heat generation; 2) The thermophysical properties of the PCM are constant in the liquid and solid phases; 3) All the PCM is initially at the same temperature and in the solid state; 4) The thermal resistance of the PCM container wall is neglected; 5) The volume change involved in the phase change is neglected; 6) There is no natural convection in the liquid phase of the PCM slabs.

The heat conduction equations for the melting process in the PCM slab are as follows:

$$\frac{\partial^2 T_s(x,t)}{\partial x^2} = \frac{1}{\alpha_s}\frac{\partial T_s(x,t)}{\partial t}, \quad in \quad 0 < x < s(t) \quad (solid), \tag{15}$$

$$\frac{\partial^2 T_l(x,t)}{\partial x^2} = \frac{1}{\alpha_l}\frac{\partial T_l(x,t)}{\partial t}, \quad in \quad s(t) < x < a \quad (liquid), \tag{16}$$

where $\alpha = k/\rho c_p$ is the thermal diffusivity of the PCM, $k$ is the thermal conductivity, $\rho$ is the density, and $c_p$ is the specific heat. The subscripts $l$ and $s$ refer to the liquid and solid phases respectively.

The boundary and interface conditions are:

$$\frac{\partial T_s(x,t)}{\partial x} = 0, \quad at \quad x = 0, \tag{17}$$

$$-k_l \frac{\partial T_s(x,t)}{\partial x}\bigg|_{x=0} = h(T_l(x,t) - T_c(t)), \quad at \quad x = a. \tag{18}$$

$$T_l(x,t) = T_s(x,t) = T_m, \quad at \quad x = s(t). \tag{19}$$

$$(-k_l \frac{\partial T_l(x,t)}{\partial x}) - (-k_s \frac{\partial T_s(x,t)}{\partial x}) = \rho L \frac{ds(t)}{dt}, \quad at \quad x = s(t), \tag{20}$$

where $L$ is the latent heat of melting.

The initial conditions are given by:

$$s(t) = 0, \quad at \quad t = 0, \tag{21}$$

$$T_s(x,t) = T_m, \quad at \quad t > 0. \tag{22}$$

Initially, the solid phase form of the PCM occupies the condenser. The initial temperature of the PCM is assumed to be equal to $T_c$, which is lower than melting temperate $T_m$. To initiate the melting process, the right vertical wall of the condenser is subjected to $T_w$ which is the exposed surface temperature of the PCM.

During the transient analysis, the primary coolant leaks into the control volume and provides energy to the melting material. The PCM temperature was initially raised up in the form of sensible heat and when it reaches the phase change temperature, the melting process starts. As the melting process progresses, the solid-liquid interface $s(t)$ advances from the surface towards the slab middle plane.

The coupled model considers the containment pressurization and the PCM melting process by $Q_{pcm}^{t+\Delta t}$, using the variables $T_w(t)$ and $T_c(t)$:

$$Q_{c-st}^{t+\Delta t} = Q_{pcm}^{t+\Delta t} = h_{conv}\, A_{pcm}(T_w(t) - T_c(t)), \tag{23}$$

where $A_{pcm}$ is the total heat transfer area and $h$ is the heat transfer coefficient.

## 3. Lumped models

In this work, we proposed an improved lumped parameter model for transient heat conduction, based on two-point Hermite approximations for integrals. We first introduce the spatially averaged dimensionless temperature for the solid and liquid phases, respectively:

$$T_{sav}(t) = \frac{1}{s(t)} \int_0^{s(t)} T_s(x,t)dx, \tag{24}$$

$$T_{lav}(t) = \frac{1}{a - s(t)} \int_{s(t)}^{a} T_l(x,t)dx. \tag{25}$$

The two-side corrected trapezoidal rule $H_{1,1}$ approximation was employed in the averaged temperature integrals for both the liquid and solid phases during the melting process of the slab, and the plain trapezoidal rule $H_{0,0}$ approximation was used to estimate the heat fluxes, as follows:

$$T_{sav}(t) = \frac{1}{2}(T_s(0,t) + T_s(s(t),t) + \frac{s(t)}{12}(\frac{\partial T_s}{\partial x}|_{x=0} - \frac{\partial T_s}{\partial x}|_{x=s(t)}), \tag{26}$$

$$T_{lav}(t) = \frac{1}{2}(T_l(s(t),t) + T_l(a,t)) + \frac{a - s(t)}{12}(\frac{\partial T_l}{\partial x}|_{x=s(t)} - \frac{\partial T_l}{\partial x}|_{x=a}), \tag{27}$$

$$T_s(s(t),t) - T_s(0,t) = \frac{s(t)}{2}(\frac{\partial T_s}{\partial x}|_{x=0} + \frac{\partial T_s}{\partial x}|_{x=s(t)}), \tag{28}$$

$$T_l(0,t) - T_l(s(t),t) = \frac{a - s(t)}{2}(\frac{\partial T_l}{\partial x}|_{x=s(t)} + \frac{\partial T_l}{\partial x}|_{x=a}). \tag{29}$$

Eqs. (17, 18, 26 - 29) and the interface conditions (19, 20) form a linear equation system of 8 algebraic equations for 8 unknown variables: $T_s(0,t)$, $T_s(s(t),t)$, $T_l(s(t),t)$, $T_c(a,t)$, $\frac{\partial T_s}{\partial x}|_{x=0}$, $\frac{\partial T_s}{\partial x}|_{x=s(t)}$, $\frac{\partial T_l}{\partial x}|_{x=s(t)}$ and $\frac{\partial T_l}{\partial x}|_{x=a}$. The linear equations system is solved to obtain the 8 unknowns variables in terms of the average temperatures of the solid and liquid phases $T_{sav}(t)$, $T_{lav}(t)$ and the interface position $s(t)$.

## 4. RESULTS AND DISCUSSION

### 4.1 Containment pressurization

For the simulation, released mass flow rate and enthalpy were initially validated by the conservative model of Todreas and Kazimi (2012). Numerical results were obtained for typical parameter values encountered in nuclear reactor engineering applications. The initial conditions of modeling are given in Table 1.

Table 1. Initial conditions used in simulation.

| | |
|---|---|
| Temperature (K) | 300 |
| Pressure (Pa) | $1.01\times10^5$ |
| Saturated liquid | 0.8 |
| Coolant pressure at core outlet (Pa) | $15.5\times10^6$ |
| Primary coolant water ($m^3$) | 354 |
| Contain vessel air ($m^3$) | 50970 |

Fig. 3(a) shows the distribution of fluid enthalpy within the containment over time. This is directly related to the discharge mass flow from the broken cold leg into the containment shown in Fig. 3(b). It can be seen that the fluid enthalpy and the mass flow rate decrease very rapidly, due to the rapid depressurization in the reactor vessel in the event of a loss of coolant accident.

At the end of each time step, a mass and energy balance is performed on the vapour region to determine the temperature, based on the assumption that the mixture of non-condensable gas and steam-water is homogeneous and in thermal equilibrium. The pressure and temperature variations with the time are shown in Fig. 4.

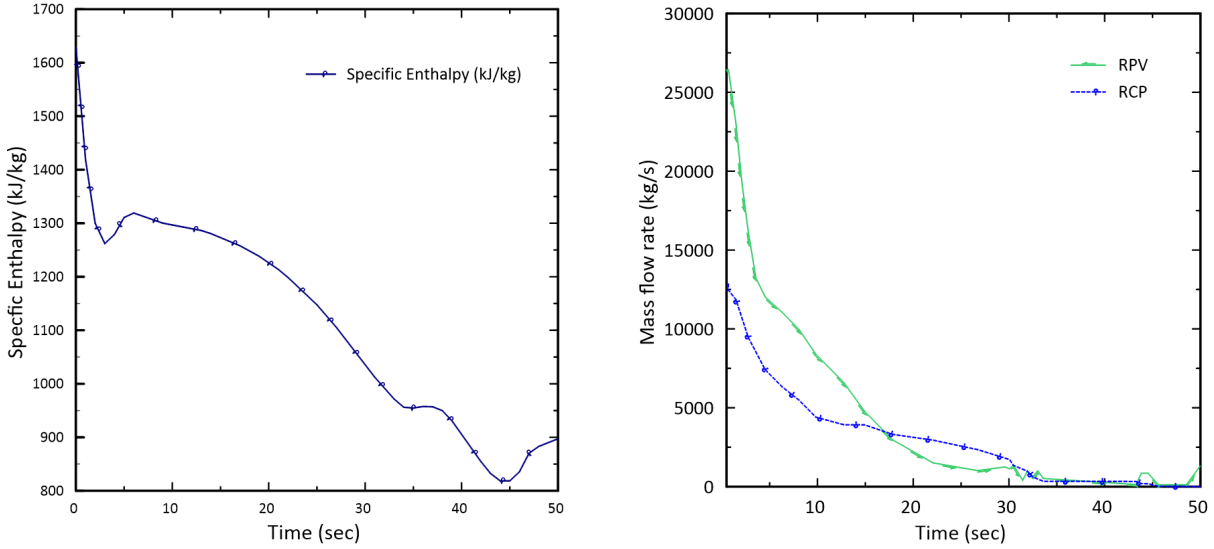


(a) (b)

Figure 3. (a) Variation of the specific enthalpy and (b) variation of mass flow rate over time of primary fluid leakage.

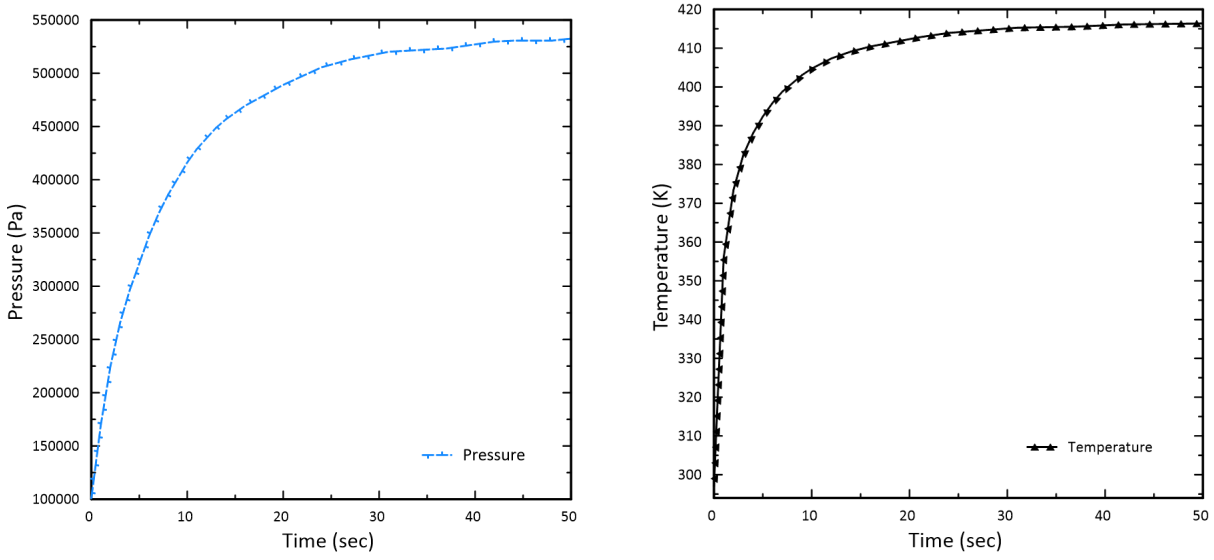


(a) (b)

Figure 4. (a) Pressure profile in the containment, (b) temperature profile in the containment.

A comparison of the simulation results with literature values (Todreas and Kazimi, 2012) is presented in Tab. 2, showing excellent agreement.

Table 2. Final conditions of the simulation.

| Final conditions | (Todreas and Kazimi (2012)) | Present model |
|---|---|---|
| Temperature (K) | 416 | 416 |
| Pressure (Pa) | $5.3\times10^5$ | $5.3\times10^5$ |
| Static quality (-) | 0.51 | 0.51 |

### 4.2 PCM melting process

The proposed model for PCM melting is validated by the comparison with an approximate analytical solution for the position of the melting front (Roday and Kazmierczak, 2009). The non-dimensionalization was carried out using:

$$\tau = \frac{\eta^2}{2St_l}\left(1+\frac{2}{Bi\eta}\right), \tag{30}$$

where:

$$\eta = \frac{S^*(t)}{a}, \quad \tau = \frac{t\alpha_l}{a^2}, \quad Bi = \frac{ha}{k_l}, \quad St_l = \frac{C_{pl}(T_a - T_m)}{L}.$$

Here $\tau$ is the dimensionless time, $\eta$ the dimensionless interface location, $St_l$ the Stefan number of the liquid, $Bi$ the Biot number, and $h$ the convective heat transfer.

The approximate analytical solution for the dimensionless temperature distribution in the liquid is given by:

$$\Theta_l\left(\xi, \eta(\tau)\right) = \frac{-Bi\xi}{1+Bi\eta(\tau)} + \frac{Bi\eta(\tau)}{1+Bi\eta(\tau)}, \tag{31}$$

where:

$$\Theta_l = \frac{T_l - T_m}{T_a - T_m}. \tag{32}$$

Here $\xi$ is the space variable.

The approximate analytical solution given by Eq. (30) and the solution obtained by the lumped parameters model proposed is shown in Fig. 5(a). A comparison between the average temperatures of the liquid obtained by the proposed lumped parameters model and the approximate analytical solution is shown in Fig. 5(b). It can be seen that the lumped model results are in excellent agreement, confirming the accuracy of the proposed model.

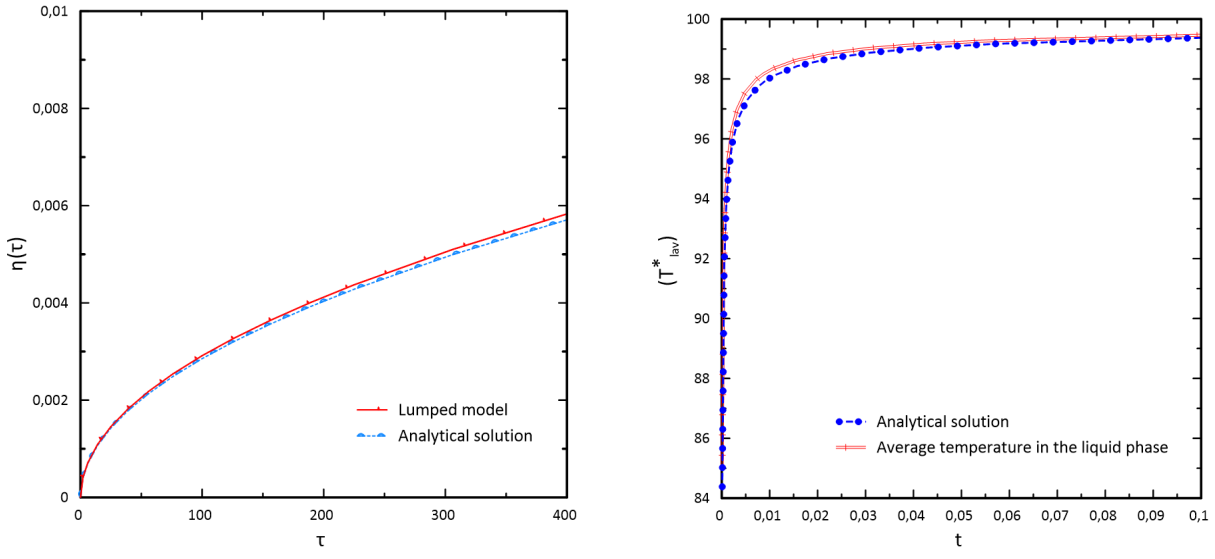


(a) (b)

Figure 5. Comparison between the lumped model and the analytical solution: (a) the interface position, (b) average temperature of the liquid.

### 4.3 Coupled model

The coupled model is proposed as a safety system measure to reduce the pressure from the containment through a condenser using PCM slabs involves a melting process. In the melting process, an immediate depressurization due to break in the cold-leg of the reactor provides energy to the PCM slabs. By carefully selecting a material that does not melt in normal operation, but only melts during accidents, heat in the containment atmosphere can be removed passively.

Materials used in thermal energy storage can be either organic materials or inorganic materials. Organic PCMs are usually more popular. They are non-corrosive and are easy to handle. In addition, organic materials are also considered to be safe, reliable and have a high latent heat (Akeiber *et al.*, 2016). Chemical stability, non-corrosive, non-explosive and low volume expansion are important issues for safety inside the containment building. Therefore, organic PCMs were chosen over inorganic materials. The thermophysical properties of organic PCMs proposed and characterized to be considered for enhancing passive safety features of nuclear containment are present in Tab. 3.

The performance of the containment using PCM slabs was analyzed computationally to test its feasibility. The initial parameters of a generic reactor selected for the simulations are presented in Tab. 4. The materials were studied by comparing different cases used in the simulation, presented in Tab. 5.

Table 3. Thermophysical properties of organic PCMs.

| PCM | RT 64 HC | RT 70 HC | RT 80 HC |
|---|---|---|---|
| Melting temperature (K) | 337 | 343 | 351 |
| Latent heat (kJ/kg) | 250 | 260 | 220 |
| Specific heat capacity (solid) (kJ/kg) | 2 | 2 | 2 |
| Specific heat capacity (Liquid) (kJ/kg) | 2 | 2 | 2 |
| Density solid (kg/m$^3$) | 880 | 880 | 900 |
| Density liquid (kg/m$^3$) | 780 | 770 | 800 |
| Heat conductivity (W/m) | 0.2 | 0.2 | 0.2 |

Table 4. Parameters of a generic reactor.

| | |
|---|---|
| Temperature (K) | 300 |
| Pressure (Pa) | $1.01\times10^5$ |
| Saturated liquid | 1 |
| Coolant pressure at core outlet (Pa) | $15.5\times10^6$ |
| Primary coolant water (m$^3$) | 159.22 |
| Contain vessel air (m$^3$) | 36811.90 |

Table 5. Calculation cases.

| Cases | Heat transfer area (m$^2$) | Thickness (m) | PCM volume (m$^3$) |
|---|---|---|---|
| 1 | 7000 | 0.02 | 140 |
| 2 | 9000 | 0.02 | 180 |
| 3 | 14000 | 0.02 | 280 |
| 4 | 18000 | 0.02 | 360 |

### 4.4 Temperature and pressure profiles in the containment within different types of PCM

The selection of PCMs with suitable phase change temperature avoids the overpressure of the containment during the pressurization, due to the absorption of heat by the phase change material. Fig. 6(a) shows the variation of the temperature during the melting of PCM RT 64 HC. It can be seen that the temperature lies over a narrow range of 385.92 K, 384.96 K, 382.59 K and 380.70 K when the heat transfer area is, respectively, 7000 m$^2$, 9000 m$^2$, 14000 m$^2$ and 18000 m$^2$. To compare the performance of PCMs, Fig. 6(b) shows the effect of temperature with time during the melting process of PCM RT 80 HC, respectively, 386.72 K, 386.01 K, 384.24 K and 382.84 K.

Fig. 7 shows the variation of the pressure in the containment during the melting of PCM RT 64 HC, RT 70 HC and PCM 80 HC when the heat transfer area is 7000 m$^2$ and 14000 m$^2$. The comparison of results shows that the PCM RT 64 HC had the best performance among the other materials analyzed, although the differences among the PCMs analyzes are not very significant. It can be seen that a larger heat transfer area provides a bigger enhancement for a lower overpressure of the containment during the pressurization.

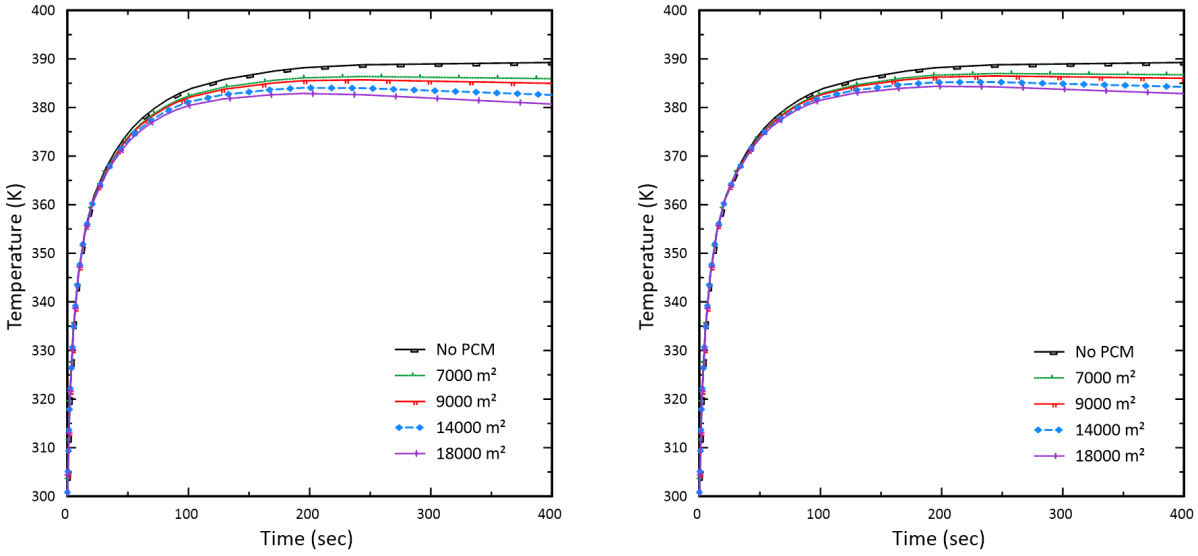


Figure 6. Temperature profiles during melting of (a) PCM RT 64 HC, (b) PCM RT 80 HC.

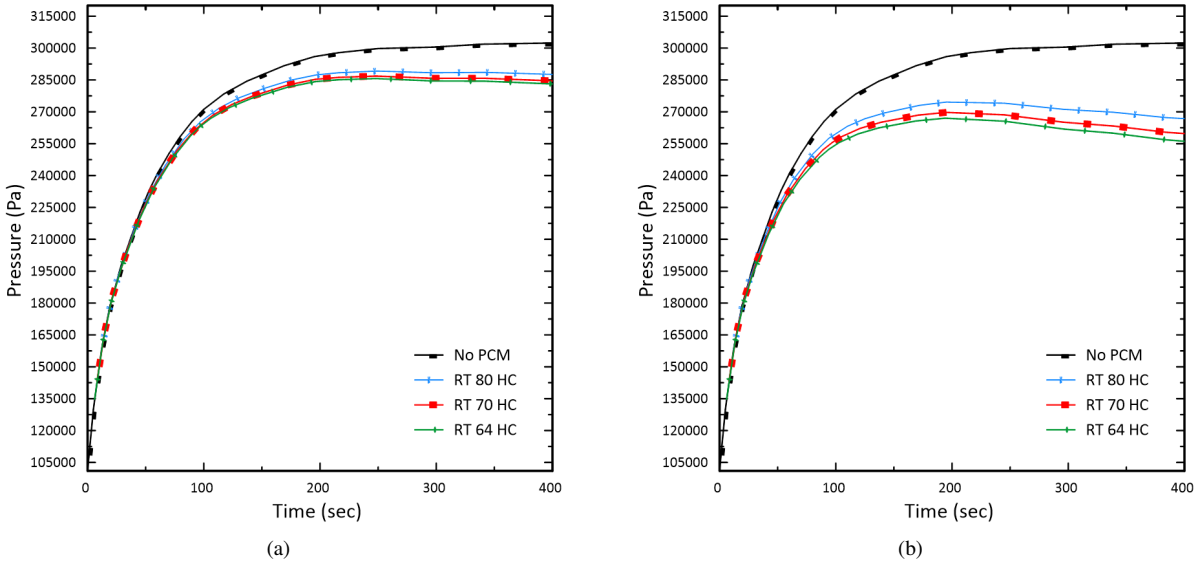


Figure 7. Pressure reduction in containment with PCM slabs: (a) 7000 $m^2$ and (b) 18000 $m^2$.

The analysis demonstrated that the PCM could successfully cool the containment under certain conditions. A comparison of the pressure reduction for all studied cases is indicated in Tab. 6.

Table 6. Total pressure reduction for all cases.

| Área | RT 64 HC | RT 70 HC | RT 80 HC |
|---|---|---|---|
| 7000 $m^2$ | $2.83\times10^5$ | $2.84\times10^5$ | $2.87\times10^5$ |
| 9000 $m^2$ | $2.77\times10^5$ | $2.79\times10^5$ | $2.83\times10^5$ |
| 14000 $m^2$ | $2.65\times10^5$ | $2.68\times10^5$ | $2.74\times10^5$ |
| 18000 $m^2$ | $2.56\times10^5$ | $2.59\times10^5$ | $2.66\times10^5$ |
| No PCM | $3.02\times10^5$ | | |

In summary, the physical requirements for a PCM are to have a suitable phase change temperature, a completely reversible melt/freeze, a large specific heat capacity, a large change in enthalpy and large thermal conductivity. The chemical requirements are small volume pressure, good compatibility with other materials, chemical stability, physical stability and non-toxicity.

### 4.5 Energy balance

A performance comparison of the mass required to cool the containment in the event of a loss of coolant accident demonstrated that the PCM RT 70 HC was more effective. Fig. 8 shows that the PCM RT 70 HC required 129059 kg to lower the maximum pressure containment. There is a difference of approximately 3172 kg and 13689 kg between the mass required of PCM RT 64 HC and PCM RT 80 HC. From the study results, it could be seen that the mass required decreased with the increase of the latent heat, as expected.

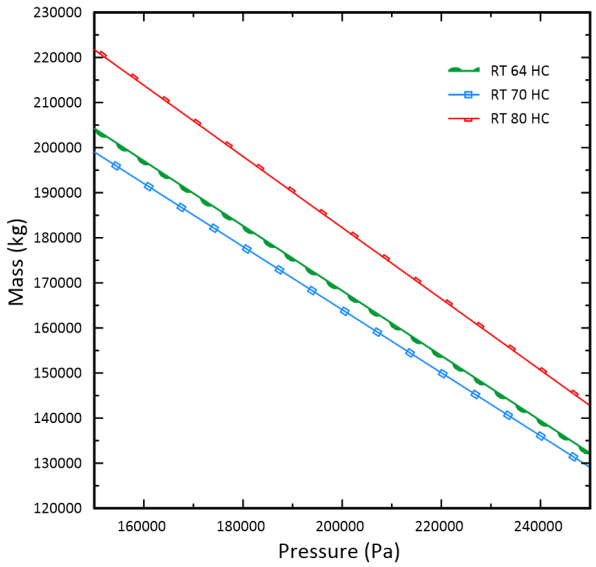


Figure 8. A performance comparison of the mass required to cool the containment.

Low thermal conductivity is considered to be a major issue for most PCMs and can be a challenge for the application of PCMs in passive cooling systems. However, it is possible to improve the thermal conductivity by developing a composite of PCM with porous metal and using a nano-materials application capable of enhancing micro-convection. Microencapsulation technology can also provide high thermal cycling stability, relative constant volume, and large heat transfer area for PCM-based thermal storage (Akeiber *et al.*, 2016).

## 5. CONCLUSION

In this study, a passive containment pressurization system using slabs of phase change materials (PCMs) has been modeled. The presented study focused on organic PCM for a passive storage system, due to its high heat of fusion, considerable compatibility with the building envelope materials and chemical stability. The proposed mathematical model consists of a conservative single-cell thermodynamic model for the mass and energy balance in the containment, and an improved lumped parameter model for one-dimensional heat conduction with the melting of a PCM slab, based on Hermite approximations for integrals. By comparing the results in the numerical pressurization model with literature data (Todreas and Kazimi, 2012), it is shown that the single cell model can predict the average temperature and pressure profiles in the containment. The lumped parameter model for one-dimensional heat conduction with the melting of a PCM slab was validated by comparing the PCM melting interface and the average temperature of the liquid phase with an approximate analytical solution (Roday and Kazmierczak, 2009). Numerical results show that the PCM RT 64 HC provided the best performance among the PCMs analyzed. In summary, the results demonstrated that even with a simple heat transfer design, the PCM could successfully cool the containment and reduce the maximum pressure in the containment.

## 6. ACKNOWLEDGEMENTS

The authors are grateful to CNPQ, CAPES (PROCAD Defesa) and FAPERJ for their financial support.

## 7. REFERENCES

Akeiber, H., Nejat, P., Majid, M.Z.A., Wahid, M.A., Jomehzadeh, F., Famileh, I.Z., Calautit, J.K., Hughes, B.R. and Zaki, S.A., 2016. "A review on phase change material (pcm) for sustainable passive cooling in building envelopes". *Renewable and Sustainable Energy Reviews*, Vol. 60, pp. 1470–1497.

Avelar, A.M., Mourão, M.B., Maturana, M., Giovedi, C., Abe, A.Y., Pedrassani, R. and Su, J., 2020. "On the nuclear

safety improvement by post-inerting small modular reactor with stainless steel cladding". *Annals of Nuclear Energy*, Vol. 149.

Cho, J.O., Ko, A., Shin, S.G., Jung, H.Y. and Lee, J.I., 2021. "Preliminary feasibility study of pcm condenser for pccs of apr1400". *Annals of Nuclear Energy*, Vol. 152.

Lee, M. and Fan, C.T., 2017. "Containment pressurization and burning of combustible gases in a large, dry pwr containment during a station blackout sequence". *Nuclear Technology*, Vol. 99.

Noori-Kalkhoran, O., Rahgoshay, M., Minuchehr, A. and Shirani, A.S., 2014. "Analysis of thermal–hydraulic parameters of wwer-1000 containment in a large break loca". *Annals of Nuclear Energy*, Vol. 68.

Papini, D., Grgic, D., Cammi, A. and Ricotti, M.E., 2011. "Analysis of different containment models for iris small break loca, using gothic and relap5 codes". *Nuclear Engineering and Design*, Vol. 241.

Roday, A.P. and Kazmierczak, M., 2009. "Analysis of phase-change in finite slabs subjected to convective boundary conditions: Part i - melting". *Int. Rev. Chem. Eng.*, Vol. 1.

Saeed, R.M., Schlegel, J.P. and Sawafta, R., 2019. "Characterization of high-temperature pcms for enhancing passive safety and heat removal capabilities in nuclear reactor systems". *Energy*, Vol. 189.

Todreas, N.E. and Kazimi, M.S., 2012. *Nuclear Systems Volume I: Thermal Hydraulic Fundamentals*. CRC press, Boca Raton, FL.

## 8. RESPONSIBILITY NOTICE

The authors are solely responsible for the printed material included in this paper.